

Correction schemes for the LHC lattice at collision

T. Sen, N. Gelfand and W. Wan, FNAL, Batavia, IL 60510

Abstract

Normal form analysis and tracking results show that both normal and skew resonances are driven strongly by the non-linear fields of the IR quadrupoles. We report here on the possibility of improving the dynamic aperture by compensating these resonances with the use of correctors placed in the IRs. The effectiveness of local correction schemes in the presence of beam-beam interactions is also studied.

1 INTRODUCTION

The target dynamic aperture for the LHC at collision is 12σ at 10^5 turns. The dynamic aperture with only random errors from version 2.0 of the Fermilab and KEK error harmonics is about 11σ at 10^5 turns [1]. Systematic uncertainties and errors in the ends reduce the dynamic aperture to about 9σ at 10^5 turns [2]. Local correction schemes based on minimizing the action kick from each multipole [2] have been investigated as a means of increasing the dynamic aperture to the target value. Here we investigate a global compensation method based on minimizing low order resonances as a complementary method to improve the dynamic aperture. We also examine the efficacy of idealized versions of local correction schemes when beam-beam interactions are included.

2 RESONANCE STRENGTHS FROM TRACKING

The basic lattice was derived from MAD 5.1. In the high luminosity insertions, Fermilab error harmonics V2.0 were used for the quadrupoles in IR5 and KEK error harmonics V2.0 were used for the quadrupoles in IR1. This is the so-called “unmixed case”. Using this lattice, the program COSY INFINITY [3] was used to generate a Taylor map. The arcs are represented by 5th order maps and the IRs are represented by 9th order maps. These are concatenated to generate a single map for the lattice. The Taylor map is tracked to calculate either the dynamic aperture or amplitude growth.

Tune scans were done to identify the resonances that drive amplitude growth. Particles were placed at initial amplitudes of 3, 5 and 7 σ and their amplitude growth was recorded over 1000 turns at each tune. The tune scan was done in two ways: 1) the vertical tune Q_y was held fixed and the horizontal tune Q_x was varied, 2) Q_x was held fixed and Q_y was varied. This was done for 30 seeds.

Figure 1 shows the amplitude growth in both planes, with seed 1 for multipole errors, for a particle initially at 5σ as a result of tune scans in the horizontal and vertical

planes. In this case, the $Q_x + 2Q_y$ and $2Q_x + Q_y$ resonances are of sufficiently large widths to produce a broad resonance. The other resonance causing a large amplitude growth is the fourth order resonance $2Q_x + 2Q_y$. Figure 2 shows the results of similar scans with seed 9. Again, the third order sum resonances and the $2Q_x + 2Q_y$ resonance cause large amplitude growth.

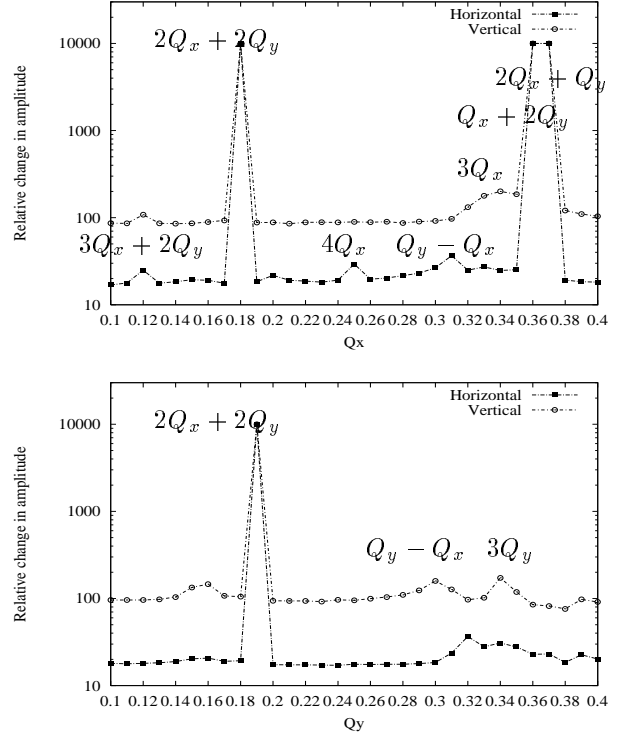


Figure 1: Amplitude growth with horizontal (top) and vertical (bottom) tune scans for seed1. For the horizontal tune scan, the vertical tune is kept constant at 0.32 while for the vertical scan the horizontal tune is kept constant at 0.31. We have identified some of the resonances that are associated with large amplitude growth. Note that the normal $Q_x + 2Q_y$ and skew $2Q_x + Q_y$ resonances have overlapped producing a broad resonance. This seed had the smallest dynamic aperture of all the seeds tracked.

In the majority of cases, the skew resonance $2Q_x + Q_y$ and the fourth order normal resonance $2Q_x + 2Q_y$ were found to cause large amplitude growth. Figure 3 shows normalized histograms over 30 seeds of the relative amplitude growth due to these resonances. For example, in about 70% of the cases the skew $2Q_x + Q_y$ resonance caused a relative amplitude growth of more than 10^4 . These tracking results show that even with the random nature of the multi-

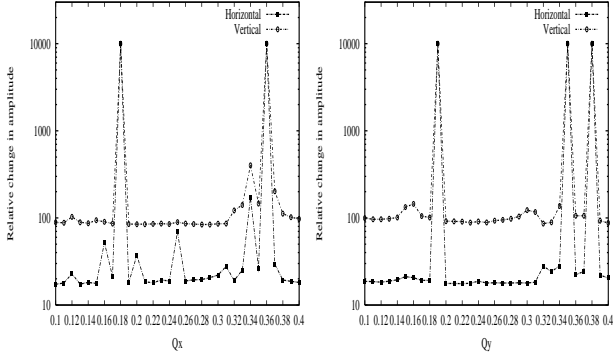


Figure 2: Amplitude growth with horizontal (left) and vertical (right) tune scans for seed9. In this case, the sum third order resonances $Q_x + 2Q_y$ and $2Q_x + Q_y$ are distinct. The dynamic aperture for this seed was near the average over all the seeds.

pole errors, the same, relatively few, low order resonances are responsible for amplitude growth. This encourages the hope that compensating these resonances may increase the dynamic aperture. At the nominal tunes ($Q_x = 63.31$, $Q_y = 59.32$), the 4th order resonance $2Q_x + 2Q_y = 245$ should not be excited. In this paper we choose to minimize only third order resonances.

3 RESONANCE STRENGTHS FROM NORMAL FORMS

The normal form \mathcal{N} of a map \mathcal{M} is obtained via

$$\mathcal{N} = \mathcal{A}^{-1} \mathcal{M} \mathcal{A} \quad (1)$$

where

$$\mathcal{A} = e^{F} \quad (2)$$

The notation $::$ signifies a Poisson bracket operation. The generating function F of the similarity transformation is

$$F = \sum_{j,k,l,m} f_{jklm} J_x^{(j+k)/2} J_y^{(l+m)/2} e^{-i\psi_{j,k,l,m}} \quad (3)$$

where $\psi_{j,k,l,m} = (j-k)(\psi_x + \psi_{x,0}) + (l-m)(\psi_y + \psi_{y,0})$. and J_x, J_y are the linear actions. The resonances of order $n = |j-k| + |l-m|$ are $n_x Q_x \pm n_y Q_y \equiv (j-k)Q_x \pm (l-m)Q_y = p$. These resonances also appear in higher orders $n+2, n+4, \dots$ in the generating function. The strength of an n th order resonance is taken to be the absolute value of the complex generating function.

$$\mathcal{F}(n_x, n_y) = \left| \sum_{\substack{j,k,l,m \\ j-k=n_x, l-m=n_y}} f_{jklm} J_x^{(j+k)/2} J_y^{(l+m)/2} e^{-i\psi_{j,k,l,m}} \right| \quad (4)$$

COSY INFINITY is used to generate the normal form of the map and also evaluate the resonance strengths.

Third order resonance strengths, both normal and skew, were calculated at an amplitude of 8σ , close to the dynamic

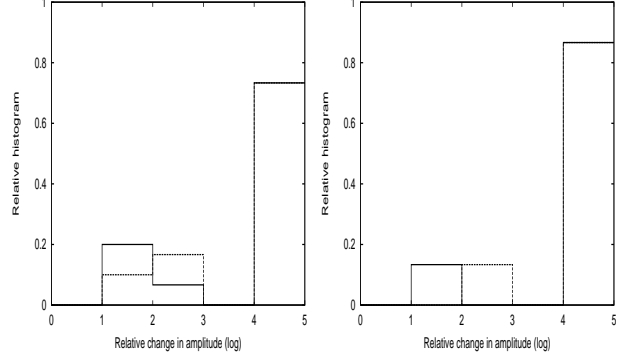


Figure 3: Normalized histograms of the relative amplitude growth (shown on a log scale) due to the resonances $2Q_x + Q_y = 186$ (left) and $2Q_x + 2Q_y = 245$ (right). The histograms represent data from tracking with 30 seeds. For example, in more than 70% of the cases, the $2Q_x + Q_y = 186$ resonance leads to a 10^4 fold or larger amplitude growth.

aperture. These resonance strengths included the contributions from higher order multipoles (the “sub-resonance” contributions). For example, the resonance $Q_x + 2Q_y$ has primary contributions from b_3 and subsidiary contributions from b_5, b_7, b_9 . Similarly the skew resonance $2Q_x + Q_y$ has primary contributions from a_3 and subsidiary contributions from a_5, a_7, a_9 .

4 CORRECTION WITH SEXTUPOLES

Correcting all four third order sum resonances $3Q_x, Q_x + 2Q_y, 2Q_x + Q_y, 3Q_y$ requires two sextupoles for each resonance or eight in all. In order to minimize the sextupole strengths, the phase advance between the sextupoles correcting a resonance have to be chosen appropriately. For example, the optimal phase advances between the sextupoles correcting the $Q_x + 2Q_y$ resonance satisfy $\Delta\psi_x + 2\Delta\psi_y = \pi/2$. In this case the corrector strengths are minimal and both the real and imaginary parts of the driving term can be corrected. However in the study reported here, we restricted ourselves to placing sextupole correctors in the MCBX and MCQS packages in the IRs. The phase advances between them are odd multiples of π and therefore far from optimal. The β functions in these correctors however are larger than they would be for sextupole correctors placed in the arcs.

In IR1 and IR5, normal sextupoles, labelled NS1,...NS4 in Figure 4, are placed in MCBX packages between Q2a, Q2b and after Q3 on both sides of the IP for a total of eight normal sextupoles. Within a single IR, the normal sextupoles in a family e.g. NS1, -NS1, are placed at locations of nearly equal beta functions in both planes and have the same strength but with opposite signs. Their contribution to the linear chromaticity is therefore zero while the phase advance between them is nearly π . A total of four sextupole strengths are available to correct the real and imaginary parts of the two normal resonances. Skew

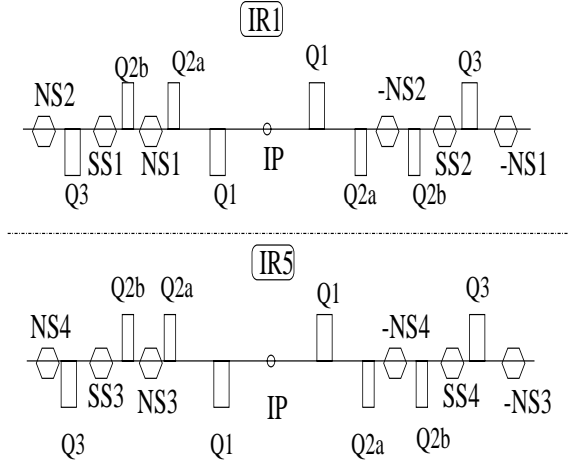


Figure 4: Placing of the 4 families of sextupoles for reducing the third order resonance strengths.

sextupoles, labelled SS1,... SS4 in Figure 4, are placed in MCQS packages after Q2b, also on both sides of the IP in IR1 and IR5, for a total of four skew sextupoles to correct the two skew resonances. Equal weighting was given to these four resonances and COSY INFINITY was used to minimize these resonances using up to the maximum sextupole field of 0.067T at the reference radius of 17mm.

Table 1 shows the resonance strengths after correction as a fraction of their original values before correction for ten seeds. The resonance strength here is the absolute value of the complex driving term. In most of these cases, one or more of the resonance strengths are lowered. Reducing all the sum third order resonances does not seem possible in general with the available sextupole strengths.

The dynamic aperture was calculated after the correction of these sum resonances. Figure 5 shows the dynamic aperture in amplitude space. At each horizontal amplitude, the dynamic aperture is averaged over ten random seeds for

Table 1: Fractional change in third order resonance strengths using sextupoles, seed by seed. $f(n_x, n_y)$ is the relative strength of the $n_x q_x + n_y q_y = n$ resonance after and before correction. The last column shows the change in dynamic aperture $\Delta\langle DA \rangle$ due to these sextupoles.

Seed	$f(3,0)$	$f(0,3)$	$f(2,1)$	$f(1,2)$	$\Delta\langle DA \rangle$
1	0.99	0.61	0.45	0.19	0.65
2	1.07	0.75	0.57	1.42	0.19
3	0.06	1.64	0.05	0.23	2.58
4	0.97	0.81	1.01	0.98	0.31
5	0.36	1.03	0.78	30.04	0.52
6	0.35	1.91	0.94	0.17	0.59
7	0.15	0.37	1.85	0.60	-0.29
8	0.81	0.27	0.53	1.27	-0.88
9	0.41	0.50	0.61	1.34	0.20
10	1.04	0.05	1.43	2.92	0.84

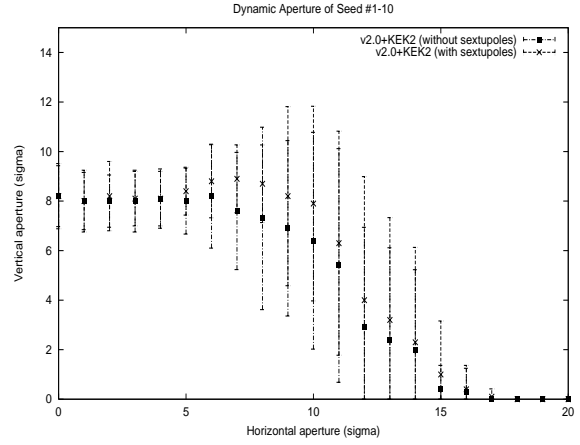


Figure 5: Dynamic aperture at different regions in amplitude space with the use of sextupoles. At each value of the initial horizontal amplitude, the dynamic aperture is averaged over 10 random seeds. There is little change in the dynamic aperture along either the x or y axis. The largest gain in dynamic aperture, about 2σ , occurs close to the diagonal.

the multipole errors. There was no improvement in the dynamic aperture along the y axis. This could be because the vertical tune is sufficiently close to the $3Q_y$ resonance that reducing this resonance strength by factors of two or less is not sufficient to improve the dynamic aperture. The largest improvement is seen close to the diagonal. The improvement in dynamic aperture along the x axis is also small.

In those cases, where resonances are dramatically reduced, there is a significant improvement in the dynamic aperture. For example, with seed 3, both the $3Q_x$ and $2Q_x + Q_y$ resonances are down to about 5% and the dynamic aperture increases by 2.6σ . With seed 10, the $3Q_y$ resonance is down to 5% of its original strength while the others have increased, yet the dynamic aperture increases by 0.8σ . It is clear that overall, the gain in dynamic aperture by attempting to minimize all the sum third order resonances with the present locations of the sextupoles is only modest. It is more likely that the resonances can be better compensated if the sextupoles are placed in the arcs so that the phase advances can be chosen appropriately. Other strategies that are possible include weighting one or two of the resonances more strongly than the others in doing the resonance correction. This is being explored.

5 CORRECTION WITH OCTUPOLES

Another way to avoid excitation of dangerous resonances is to reduce the tune footprint of the beam. The tune shift with amplitude depends quadratically on the sextupole strengths but linearly on the octupole strengths. Octupoles are therefore better suited for this purpose. There are three detuning terms to be minimized: $\partial Q_x / \partial J_x$, $\partial Q_x / \partial J_y$, $\partial Q_y / \partial J_y$. Three pairs of octupoles are used with members in a pair set

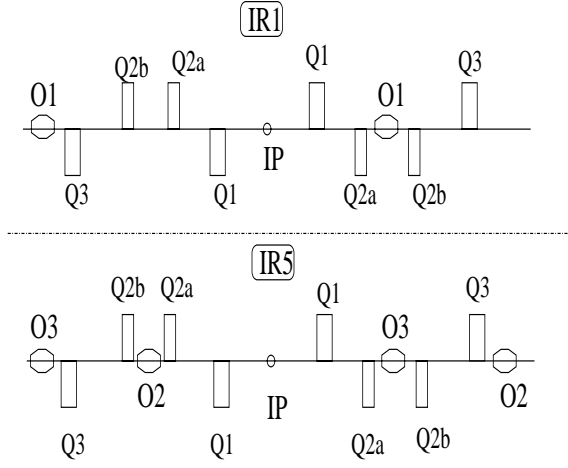


Figure 6: Placing of the 3 families of octupoles for reducing the tune shift with amplitude.

to the same strength and placed at nearly the same values of the beta functions. Members of the 3 families labelled $O1$, $O2$, $O3$ are shown in Figure 6.

The main purpose of the octupoles is to reduce the tune shift with amplitude. Figure 7 shows that the tune footprint for seed 1 is significantly smaller when the octupoles are used. However the orbit is not centered in the octupoles due to the crossing angle. Consequently they also affect the third order resonance strengths due to the feed-down into sextupole components. Table 2 shows the fractional resonance strengths after using the octupoles. The changes that occur with the octupoles are not controlled. For example, with seed 1 all the sum resonances were reduced while with seed 9, three of the four sum resonances increased in strength. In order to check that the feed-down

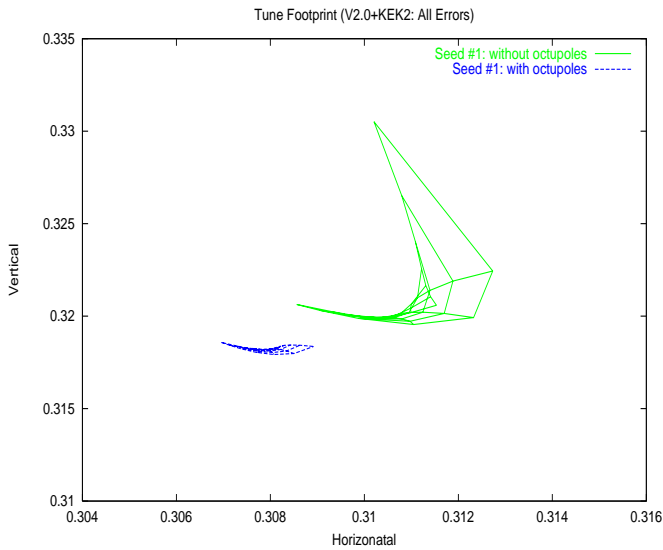


Figure 7: Tune footprint with and without octupoles for seed1.

Table 2: Fractional third order resonance strengths after reducing the tune spread with octupoles.

Seed	$f(3,0)$	$f(0,3)$	$f(2,1)$	$f(1,2)$	$\Delta\langle DA \rangle$
1	0.83	0.27	0.08	0.18	1.89
2	0.42	2.26	0.85	1.24	-1.46
3	0.34	1.87	0.49	0.22	0.55
4	3.29	0.52	4.90	0.84	0.57
5	0.86	0.83	1.30	25.70	0.04
6	0.32	1.42	0.62	0.22	0.17
7	0.09	0.55	1.93	0.62	2.61
8	2.46	0.77	0.14	1.89	1.57
9	0.57	1.19	1.52	1.23	1.65
10	1.05	0.53	0.31	1.07	-1.47

from the octupoles is responsible for the changes in resonance strengths, the octupoles were displaced transversely so that they were centered on the closed orbit. In this case, there was no change in the third order resonance strengths.

Figure 8 shows the average dynamic aperture over 10 seeds with and without the use of octupoles. The average increase in dynamic aperture with the use of the octupoles is somewhat greater than that obtained with the sextupoles. In particular, the dynamic aperture also increases along the y axis. Reducing the tune shift at large amplitudes therefore appears more beneficial in avoiding the effects of the $3Q_y$ resonance.

6 SEXTUPOLES AND OCTUPOLES TOGETHER.

When both sextupoles and octupoles are used, a two step procedure is necessary. Due to the fact that octupoles

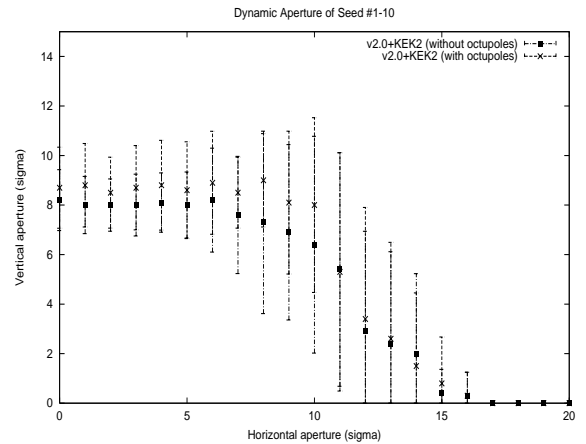


Figure 8: Dynamic aperture at different regions in amplitude space with the use of octupoles. At each value of the initial horizontal amplitude, the dynamic aperture is averaged over 10 random seeds. The octupoles help to increase the dynamic aperture along the y axis as well as close to the diagonal.

Table 3: Fractional third order resonance strengths after correction with octupoles and sextupoles.

Seed	f(3,0)	f(0,3)	f(2,1)	f(1,2)	$\Delta\langle DA \rangle$
1	0.49	0.18	0.07	0.10	2.69
2	0.47	1.74	0.72	1.40	-1.03
3	0.24	3.35	0.40	0.16	0.22
4	2.67	0.59	2.02	1.09	0.75
5	0.33	0.93	0.94	49.87	0.41
6	0.33	1.32	0.55	0.22	-0.10
7	0.12	0.14	0.29	0.48	2.49
8	1.31	0.98	1.48	1.58	1.69
9	0.48	0.97	1.29	0.98	2.22
10	0.74	0.07	1.07	1.42	0.49

change the third order resonance strengths via feed-down, it is difficult to do a simultaneous compensation of resonance strengths and tune shifts with amplitude. In the two step procedure, first octupoles are used to reduce the tune footprint and a new map of the lattice is obtained with these octupole correctors. The third order resonances of this new map are then compensated with sextupoles.

Table 3 shows the fractional resonance strengths after correction with the octupoles and sextupoles. Compared to the fractional strengths shown in Table 2, most of the resonance strengths have decreased. For example, with seed 1 the $3Q_x$ resonance is reduced to nearly half its value with octupoles alone and the increase in dynamic aperture changes from 1.89σ to 2.69σ .

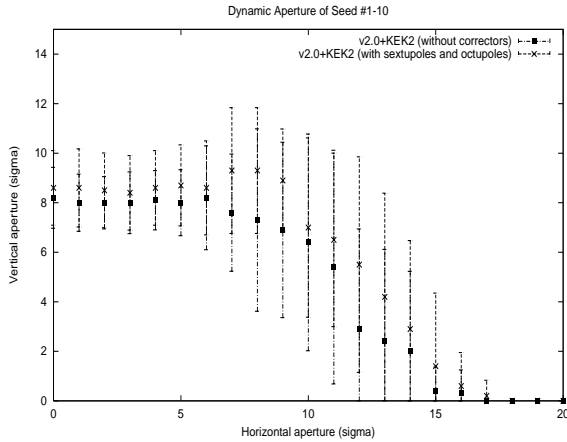


Figure 9: Dynamic aperture at different regions in amplitude space with the use of sextupoles and octupoles. At each value of the initial horizontal amplitude, the dynamic aperture is averaged over 10 random seeds. As with octupoles alone, sextupole and octupole correctors help to improve the dynamic aperture at almost all angles in physical space.

Figure 9 shows the average dynamic aperture over 10 seeds with and without the use of sextupoles and octupoles. Again, as was the case with only octupoles, there is some

improvement in the dynamic aperture along the y -axis. Overall, the gain in dynamic aperture is larger than with either sextupoles or octupoles alone.

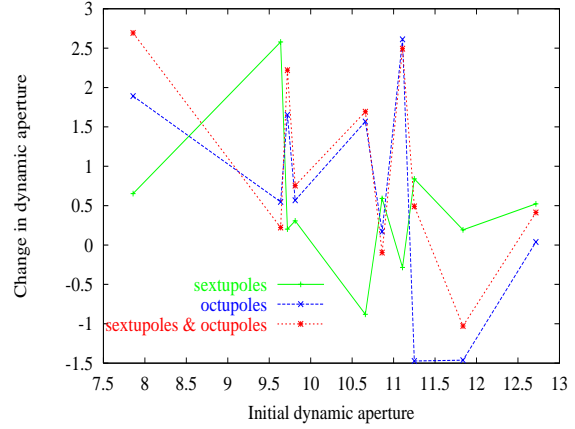


Figure 10: The change in dynamic aperture as a function of the initial dynamic aperture for each of the correction schemes.

Figure 10 shows the change in dynamic aperture as a function of the initial aperture for the different schemes. It is clear that the variation in dynamic aperture from seed to seed due to the action of the sextupoles is quite different from the variation due to the octupoles. For example, the maximum increase with sextupoles occurred with seed 1 while the maximum with octupoles occurred with seed 7. Octupoles were most effective in increasing the smallest dynamic aperture (seed 1). In almost all cases, the addition of sextupoles to octupoles helped improve the quality of the correction.

Table 4: The dynamic aperture (DA) with the use of low-order correctors. $\langle DA \rangle$ is calculated after 10^3 turns and averaged over 10 random seeds for the multipole errors. The last column shows the maximum increase in DA over these seeds with the use of the correctors.

Correction	$\langle DA \rangle \pm \sigma_{\langle DA \rangle}$	Max $\Delta\langle DA \rangle$
No correction	10.5 ± 1.4	
Sextupoles	11.0 ± 1.4	2.58
Octupoles	11.2 ± 1.4	2.61
Sextupoles & octupoles	11.5 ± 1.2	2.69

Table 4 summarizes the change in the dynamic aperture, averaged over emittance space and 10 seeds, obtained with use of the low order correctors. On average, the sextupoles increase the dynamic aperture by 0.5σ , octupoles by 0.7σ and the two together by 1σ . These schemes can be improved. One possibility is to identify the important resonances, seed by seed, and compensate only those resonances. For the preliminary study reported here, we compensated all the third order sum resonances for every seed. Lower order resonances such as the second order

Table 5: Idealized versions of the local correction schemes 2 and 4 where the systematic and random values of the specified multipoles are set to zero. Tracking calculations in this paper did not include the systematic uncertainties (db_n, da_n).

Scheme	Zeroed random multipoles
2	$(b_3, b_4, b_5, b_6) \text{ \& } (a_3, a_4, a_5, a_6)$
4	$(b_3, b_4, b_5, b_6, b_{10}) \text{ \& } (a_3, a_4, a_5, a_6)$

$Q_y - Q_x$ resonance also appear to be associated with amplitude growth (seen in Figures 1 and 2). This is one of several resonances that can be compensated by octupoles.

7 LOCAL CORRECTION SCHEMES WITH BEAM-BEAM

Beam-beam interactions have a significant impact on the dynamic aperture [1]. We have examined the impact of idealized versions of local correction schemes when beam-beam interactions are included. In the idealized versions we set to zero the systematic and random value of the specified multipoles. Table 5 shows the local correction schemes 2 and 4 as proposed in [2]. In practice, the local correction schemes will not be quite as effective as the idealized versions used here.

The tracking results reported in this section, both with and without beam-beam interactions, were done with the program TEVLAT [4]. The lattice was also derived from MAD5.1 but the IR quadrupoles were mixed, i.e. Fermilab error harmonics V2.0 were used in Q2a, Q2b and KEK V2.0 were used in Q1 and Q3.

In order to be consistent in evaluating the correction schemes, we will compare the dynamic aperture with and without the beam-beam interactions at the same number of turns. We have found that when the beam-beam interactions are included, particles must be tracked for a minimum of 10^5 turns in order to get meaningful results [1]. It is important to note that the dynamic aperture with beam-beam interactions drops faster with the number of turns than without.

Figure 11 shows the dynamic aperture for five seeds with and without the beam-beam interactions when no correction is applied.

Figure 12 shows the dynamic aperture in both cases with the idealized scheme 2. The dynamic aperture with the beam-beam improves by about 1σ compared to the case when no corrections are applied. As expected, the improvement is smaller compared to the case when the beam-beam interactions are not included.

Figure 13 shows the dynamic aperture in both cases with the idealized scheme 4. In this case, the dynamic aperture without beam-beam improves dramatically by about 4.7σ compared to the case without correction. When the beam-beam interactions are included, the dynamic aperture increases by 3.2σ to 12.4σ . This scheme is clearly

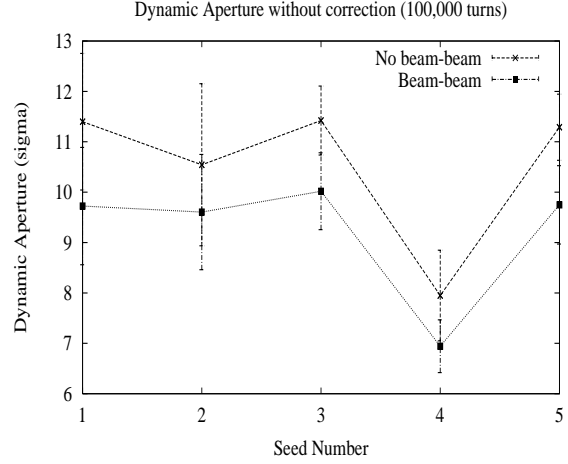


Figure 11: Dynamic aperture with and without the beam-beam interactions without any correction. Particles are tracked for 10^5 turns over 10 angles in emittance space. The average reduction in dynamic aperture due to the beam-beam is 1.3σ .

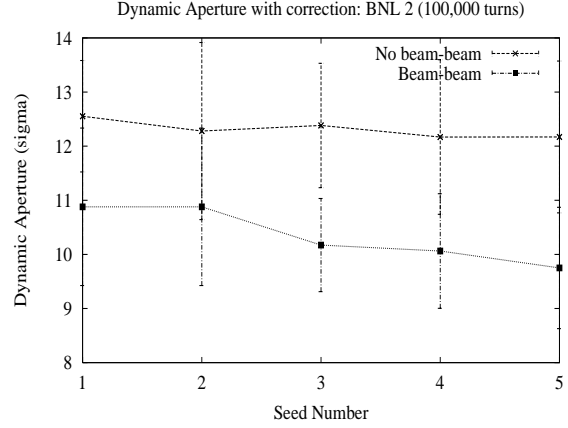


Figure 12: Dynamic aperture with and without the beam-beam interactions with the idealized local correction scheme 2. Particles are tracked for 10^5 turns over 10 angles in emittance space.

quite effective in improving the dynamic aperture, albeit by a smaller amount, even when the beam-beam interactions are included. Most of the increase is due to eliminating the large $\langle b_{10} \rangle = -0.25$ contribution to the dynamic aperture.

Table 6 summarizes the average change in dynamic aperture with and without the beam-beam interactions for the different correction schemes.

8 SUMMARY

Using only sextupoles and octupoles in IR1 and IR5 we attempted to increase the dynamic aperture. These multipoles were used to compensate sum third order resonances and reduce the tune shift with amplitude. Ten random seeds were used for the multipole errors. Averaged over the

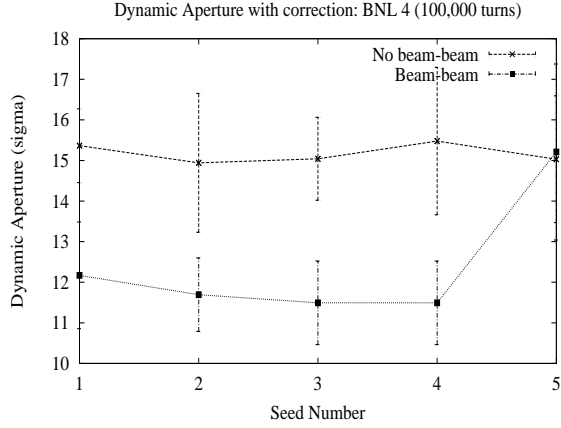


Figure 13: Dynamic aperture with and without the beam-beam interactions with the idealized local correction scheme 4. Particles are tracked for 10^5 turns over 10 angles in emittance space.

seeds, these multipoles increased the dynamic aperture by about 1σ . The maximum increase in dynamic aperture over these seeds is 2.7σ . This increase is encouraging because it demonstrates that resonance compensation works in principle. Our use of the sextupoles was constrained by placing them in the IRs. The relevant phase advances between these sextupoles correcting a resonance is an odd multiple of π while at optimal locations these phase advances would be odd multiples of $\pi/2$. This can be achieved by placing the sextupole correctors in the arcs. Resonance compensation may be further improved by first doing a more detailed search for the important resonances at the working point, using the method of frequency analysis for example. Low order coupling resonances such as $Q_y - Q_x$ may require a dedicated compensation. Important resonances of higher order than third will require higher order multipoles. We believe that resonance compensation can be a useful complement to the local correction scheme.

We have also investigated the efficacy of idealized versions of the local correction schemes when beam-beam interactions are included. As expected, the increase in dynamic aperture is not as large compared to the case when beam-beam interactions are not included. However the in-

crease with scheme 4 (where $b_{10} = 0$) is still significant, about 3σ . This demonstrates that the local correction can still be very useful, even in the presence of the beam-beam interactions. We believe that in order to improve upon the local correction, compensation of the beam-beam driven resonances should be investigated.

9 REFERENCES

- [1] T. Sen, N. Gelfand, C. Johnstone, W. Wan, *Effect of the beam-beam interactions on the dynamic aperture and amplitude growth in the LHC*, Proc. CERN Beam-beam Workshop, April 1999
- [2] J. Wei et.al., *Interaction region local correction for the LHC*, PAC 1999
- [3] M. Berz, COSY INFINITY Version 7, Technical report MSUCL-977 revised. National Superconducting Cyclotron Laboratory, Michigan State University, 1996
- [4] A. Russell, private communication

Table 6: Average dynamic aperture without and with beam-beam and different idealized local correction schemes. The dynamic aperture is calculated after 10^5 turns and averaged over 5 random seeds. No systematic uncertainties db_n, da_n are included.

Correction Scheme	No Beam-Beam $\langle DA \rangle \pm \sigma_{DA}$	With Beam-beam $\langle DA \rangle \pm \sigma_{DA}$
No correction	10.52 ± 1.04	9.21 ± 0.88
Scheme 2	12.31 ± 1.33	10.35 ± 1.19
Scheme 4	15.17 ± 1.40	12.41 ± 1.29